HUMAN CONTROL IN ROTATED FRAMES: ANISOTROPIES IN THE MISALIGNMENT DISTURBANCE FUNCTION OF PITCH, ROLL, AND YAW

Stephen R. Ellis, Bernard D. Adelstein[1], Kiwon Yeom[2]
NASA[1], San Jose State University Foundation[2]
NASA Ames Research Center, Moffett Field CA 94035

Comparative misalignment disturbance functions (MDF) have been measured for rotations between display and control axes for pure pitch, roll, and yaw misalignments in a high fidelity virtual environment. Twenty participants manually moved a virtual cursor using position control to touch 3-dimensionally, randomly presented nearby targets having a constant Fitts Index of Difficulty. Results show a peak disturbance near 120° of rotation for all axes with Roll being distinguishably more disturbed. Some reasons for observed anisotropies, nonlinearities and an equiaxial spiral feature are briefly discussed and modeled

INTRODUCTION

Some of the earliest studies of stimulus-response compatibility were of the geometric relationship between the motion of controls and the indicators they influenced. For example, original interest focused on the relationships between the placement and rotation of control knobs and the placement and motion direction of associated dial indicators (Fitts & Simon, 1952). More recently the spatial motion of a cursor or a physically controlled element with respect to input control device orientation has been examined. (Worringhan & Beringer 1989; Cunningham & Vardi, 1990; Ellis, Tyler, Kim & Stark, 1992; Macedo, Kaber, Endsley, Powanusorn, & Myung, 1998; Ellis & Adelstein, 2009; Abeele & Bock, 2001; Wickens, Keller & Small, 2010; Chintamani, Cao, Ellis, & Pandya, 2010). This situation is frequently encountered in teleoperation when the coordinate systems for motor control and visual feedback are misaligned, e.g., Smith & Smith, 1962; Smith, Henning & Li, 1998. Suitable sensors and telemetry from the remote system can provide data to correct the users' control coordinates[1] so that all displayed motion is parallel to the users' physical input motion (e.g. Intuitive Surgical's *da Vinci* surgical robot). However, it is often the case that this signal processing is not possible. Correction of rotated control frames is also problematic since users may be required to visualize motion in multiple rotated input frames simultaneously, for example, as in the Space Station Remote Manipulation System.

A final issue associated with rotated control frame corrections arises due to the correction essentially being a type of partial automation. Since such automation can fail, users need practice to work without it. The failure of the infrastructure correcting rotated controls frames is analogous to failure of a telerobot resolved control system, which could necessitate that the operator fall back to a joint angle control technique (Sheridan, 2002, pp. 61-64). Accordingly, both for training and task definition, the cause of users' task difficulties associated with operation during control frame rotation needs to be understood.

Though the telerobot control misalignment problem occasionally has been studied with respect to the users' pitch, roll, and yaw control coordinates (e.g., Smith & Smith, 1962), most previous studies have been of yaw angle misalignment. Moreover, there have been no comparative studies of large ranges of misalignment in all three canonical misalignment axes.

We call the function describing this disturbance due to rotation of the users' control axes the Misalignment Disturbance Function (MDF). Indeed, to the authors' knowledge there is no truly analytic, computational theory predicting the MDF that takes into account both the specific geometry of the misalignment and the location of targets for the intended movement (c.f. Wickens et al., 2010). As considered briefly in the discussion, such a theory will need to reference the geometric features of the rotation, e.g. the rotation axis. We believe that the specific shape of the disturbance function will also be important to developing this theory of user response to control-display misalignment.

The following study is a step towards establishing the detailed shape of the MDF for pitch, roll, and yaw misalignments between 0° and 180° collected within a comparable environment. This initial descriptive study is to the authors' knowledge the first time such a set of rotations has been studied with precision sufficient to foster a theoretical development. Significantly, we have elected to study only the motion effects due to the rotation and avoided introducing cues to the local coordinates of the cursor under the subjects' control, a restriction that will lead below to an observation that is one of this study's findings.

METHODS

Subjects

Twenty subjects aged from 18 to 64 (12 men and 8 women) participated. All were unpaid volunteers, including the three authors who were included since no specific empirical hypothesis was being tested. Prior to participation, all provided their informed consent to a protocol approved by the NASA Ames Institutional Review Board. All participants were then screened for normal stereo acuity, measured for interpupillary distance to adjust the stereo display software, and provided written instructions for the experiment. Eighteen self-reported to be right-handed, two were left-handed.

Head mounted display: A Rockwell-Collins SR80™ head mounted display (HMD) was used to view the experimental environment. This particular display was modified by the manufacturer to include a centered, circular (10° diameter), binocular see-through region. While this modification enabled operation in an augmented-reality mode, it served in the present experiment solely to assist the mechanical alignment of the HMD's exit pupil, the participants' eyes, and the eye points of the stereo display software. The HMD provided 53° (Vertical) x

---
[1] This situation is a case of Sheridan's (2002, p. 149) Roseborough dilemma.

63° (Horizontal) field-of-view images at SXGA (1280 x 1024 pixel) resolution to each eye with full-binocular overlap at a fixed 0.25-D (4 m) focus. HMD images were produced by 60-frame/s, reflective (FLCOS) elements with field-sequential color at a 100:1 contrast ratio and a luminance range of ~15 to ~150 cd/m^2. The HMD was used in an immersing, closed mode by darkening the room such that real physical elements in the experiment room were generally not visible in the see-through region. Nonetheless, dim reflections from the hand tracker held by the participants were useful during familiarization to help them learn to localize the physical start point from which all experiment movements had to be made.

Computer hardware and software: A six-core 3.2-GHz Dell Precision PWS760 workstation operating Windows-XP (SP2) ran all experiment software. A custom written C++ virtual environment (VE) application, specified by the first author and developed in-house by Richard H. Jacoby, generated the stereoscopic VE and controlled the progress of the experiment via the WorldToolKit (Sense8, Inc.) software framework. The VE retrieved head and hand position and pose measurements that were deposited in shared memory by stand-alone tracker application software (AuAST, AuSim, Inc.) running as a Windows service. These measurements were made by a pair of synchronized Polhemus FasTrak sensor units, each with a transmitter and single receiver updated at 120 frames/s, one unit for the head and the other for the hand. This shared-memory dual-FasTrak configuration, combined with external timing firmware, enabled high temporal fidelity rendering of the polygonal images depicted in Figures 1 and 2 at a stable, full-system latency measured at ~25 ms (Hill, Adelstein & Ellis, 2004). The HMD, the component in our system with the slowest refresh, limited our simulation to a constant 60 frame/s update rate.

User response button and trackers: As noted above, participant head position and orientation were tracked with a 6-degree-of-freedom electromagnetic sensor rigidly attached to the HMD. The position of the 3D cursor within the experimental VE was determined by the position of a second sensor held in the participants' dominant hand. Raw position and orientation reports were adjusted through a calibration mesh to achieve translational and rotational accuracies better than 5 mm and 0.25°, respectively, within the volume experimentally used. Button presses on an instrumented three-button handle held in the participants' nondominant hand provided feedback to start trials, indicate responses, and advance the experiment.

The virtual experimental environment: The experimental VE created for the study was a simple room with dimensions roughly matching the actual room (4.0 x 4.5 x 2.9 m) in which the experiment was conducted. Some realism was provided by texture mapping the ceiling and ground planes to roughly correspond to those in the physical room. Diffuse lighting coming from virtual room ceiling mimicked the lighting in the real room.

Five different graphic objects, as follows, were located in the virtual room and used for the experiment. 1) A blue, flat shaded, spherical 3D cursor (3 cm diameter), which was controlled by the position of the FasTrak receiver held in the participant's dominant hand. 2) A similarly shaded, larger green sphere that was presented within one of the eight possible octants with participant-specific random positions. The green sphere provided a target towards which the participants moved their cursor and was sized with respect to its distance from the start point to maintain a constant Fitts Index of Difficulty of 3.5. Target spheres were positioned to be generally visible and not require more than half a step from the participants starting location to be touched. On each trial, a target sphere appeared and remained visible until contact by the blue cursor sphere was detected, at which point the target disappeared and the trial ended. 3) A fixed-size 3-cm red cube that was also controlled by the hand-held FasTrak receiver and used only during training trials to assist participants' familiarization with the experimental task described below. 4) A smaller blue wire-frame sphere (5 cm diameter) centered at the start position indicated the movement starting location and remained visible throughout the trials. 5) A larger wire-frame yellow sphere (20 cm diameter), concentric with the blue wire frame sphere, to assist participants in finding the movement start position prior to each trial. The yellow wire-frame disappeared at the start of each trial. Figures 1 and 2, respectively, present exocentric and egocentric views of the experiment's basic VE elements.

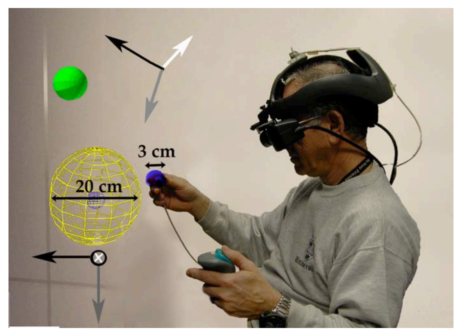

Figure 1. Composited exocentric view shows a participant moving the computer-generated blue cursor ball to touch the larger flat-shaded spherical target. The wire-frame sphere encircling the start point, shown for scale, disappeared on trial start. The two coordinate frames, not visible during testing, show a multi-axis rotational misalignment between the display (lower left) and the control axes (upper left-center).

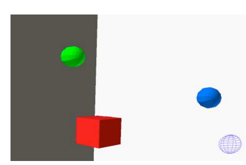

Figure 2. Screen shot of the key environmental elements as seen during familiarization. The blue, flat-shaded cursor (right) was moved to touch the green, flat-shaded target (left). As illustrated, a red cube (center), visible only during the familiarization runs but not the actual experiment, was displayed to indicate true hand position as explained in the text. The small wire-frame sphere marked the blue cursor starting point and remained visible during each movement.

Since we were not using the system in augmented reality mode, we did not attempt to precisely register the physical and virtual elements, e.g., the user's hand and the "hand held" blue cursor.

However, since we had approximate measurement of the angular and translational offset between the head sensor and the participants' eyes, we were able to subjectively confirm registration between the their hand-held sensor and the corresponding 3D graphics cursor that they controlled to within approximately 2-9 cm. This accuracy was easily adequate for our experiment since the participant did not control the cursor's orientation, only its position. The presence of the constant offset was simply perceived by the participant as if the cursor was on the end of a short wand positioned relative to their cursor control hand.

Experimental Design and Conduct

Task: The experiment was conducted in three phases. The first phase began with screening of the participant for normal stereoscopic acuity of at least 1 arcmin based on the Orthorater stereoacuity test. Pilot testing had indicated this level would be adequate for the task. Next, the participants' inter-pupilary distance (IPD)was measured with an Essilor Digital CRP that we then used to set the VE software's IPD. Participants were given a written description of the experiment and provided several minutes to read it. Participants were familiarized with the HMD and its donning procedure by watching the experimenter put it on and center his eyes in the exit pupils.

Once in the equipment, participants tried the movement task using the red familiarization cube while moving the blue spherical cursor to touch the green target spheres. The task required that the cursor be positioned at the start point so that a button press by the nondominant hand would trigger the disappearance of the large yellow centering wireframe and the appearance of a green target sphere. Participants were told to try *to make a smooth coordinated movement as quickly and comfortably as possible* from the start point to the target. We recorded and time-stamped the complete trajectory of each movement. Upon contact with the cursor, the target would disappear and the large centering wireframe would reappear to cue the subject to begin the next trial and make the next movement. After several movements illustrating zero rotational misalignment between the control and display coordinates and then several with rotations of varying difficulty, the simulation was restarted and run without the familiarization cube, but with sample control-display rotations. This provided the participants with practice in finding the start location in the physical room and performing the task.

The second phase, the actual practice of the experiment's targeting task, began with the participants repeating the HMD donning and alignment and task familiarization. One significant aspect of this practice phase was that control-display coordinate rotations were presented in basic blocks of ten movements as they would during the actual experiment trials. The first three targets of each block of ten were presented directly in front of the participant within arm's reach in a horizontal row from left to right. For these three targets participants were encouraged to informally explore the nature of the rotation before touching the target, taking as much time and making as many movements, typically up to ten, as needed to understand the nature of the rotation they would have to deal with while acquiring the block's remaining seven targets.

The three warm-up targets were intended to reduce inter-rotation transition effects. The trajectories to these warm-up targets were not analyzed because these movements frequently contained many restarts and probing motions made to identify the nature of the control-display rotation. Because the experiment switched between *axes* of control-display rotation after large blocks every 100 trials (ten basic blocks), the three warm-ups also served to mitigate possible rotation axis transition effects. While three movements were deemed sufficient to allow classic asymmetric transfer effects to abate (Poulton, 1974), we in fact had many more due to the participants probing of the rotation. Note that because only seven target movements were distributed among the eight octants, each subject had a randomly determined octant in which no target appeared.

During phase three, the actual experiment, each of the three rotation axis conditions typically took 20-35 minutes to complete. With generally 5 to 10-minute breaks between axis conditions, screening and familiarization, the overall experiment took each participant 2-3 hours to complete.

Independent variables: Three independent variables and associated levels were used in this study. 1) *Axis of the misalignment rotation* (3 levels): *Pitch* about the +*y*-axis to the participants' right; *Yaw* about +*z*-axis directly downward, and *Roll* about +*x*-axis directed straight ahead. All axes were fixed with respect to the real laboratory frame and correspond to standard aeronautical coordinates for a standing subject looking straight ahead along the + *x*-axis, 2) *Amount of rotation* about each of the axes (10 levels): 0°, 20°, 45°, 60°, 75°, 90°, 105°, 120°, 140°, and 180° about each of the axes, presented with participant-specific random sequences, 3) *Sequence of rotation axis selection* (6 levels): Each of the six possible sequences, e.g. Pitch-Yaw-Roll, was assigned to subgroups of three subjects to produce balanced independent groups that could be used to examine sequence effects. Two extra subjects were later included as their data did not affect the planned ANOVAs. The direction of rotation about each axis (clockwise or counterclockwise) was balanced across all subjects but ignored for analysis. Randomizations were filtered to prevent back-to-back repetition of the same condition.

Dependent variables: The following two raw dependent measures were employed: Movement Time (MT, s) & Path Length (PL, cm) from start to target contact.

RESULTS

Some sample trajectories for roll and yaw axis rotation from one participant are presented in Figure 3. The complex trajectories evident during movement associated with larger rotations demonstrates the challenges for their analysis. We are currently working on a rectification, normalization and filtering technique to develop an averaging process similar to one previously used for similar movements in two-dimensions (Ellis & Adelstein, 2009). For the present descriptive study we have elected to simply exclude from analysis those movements for which it was evident that the participants were unable to accomplish the task because they became very disoriented. For this purpose, we developed a technique (Yeom. Adelstein, & Ellis, 2012) to count the discontinuities in the movements that we employed to identify 91 (1.5%) movements to exclude from analysis. Fortunately, because of replications we were able to conduct several useful analyses, but we note that the loss of frame of reference needs to be managed because otherwise analyses can become very distorted by extreme values, literally orders of magnitude different from most measurements. We address also this problem below with a nonparametric analysis.

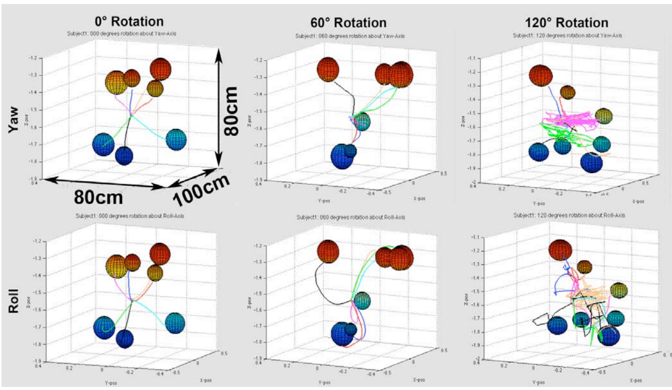

Figure 3. Sample subjects individual movements.

Since individual participants' performance on the task varied widely, by a factor of ~3, even after exclusion of the extreme cases due to complete disorientation[2], we found support for initial plan to use a repeated-measures experiment design with accommodation for possible interfering transfer effects, avoiding the need for large numbers of subjects per group.

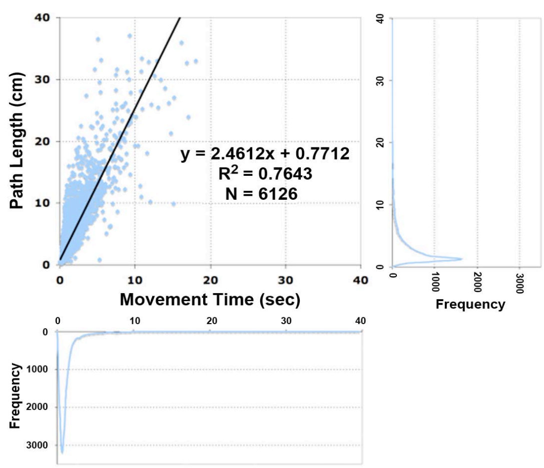

Figure 4. Scatterplot of Movement Time and Path Length with marginals

Figure 4 represents the statistical distribution of our two dependent variables as well as their correlation. We can see from the marginal distributions that both are highly positively skewed as well as positively correlated. Because of the possibility that the two measures could reflect a varying speed-accuracy tradeoff during the course of each subject's testing, we plan future analysis once suitable normalized rescalings of each variable can be identified.

The very strong skew and kurtosis in the Movement Time data argue for the need for a corrective transformation before attempting an Analysis of Variance (ANOVA). We found than a log(1+*t*) transform adjusted raw data skew from 6.891 to 0.8090 and kurtosis from 83.98 to 0.3492, suitably correcting the statistical properties to permit ANOVA.

We employed the |STAT(http://hcibib.org/perlman/stat/) statistical package to compute analyses of variance on the transformed data. First, no significant effect of the sequence of rotation axis was found in an independent groups analysis for sequence effects using all 20 subjects ($F(5,14)=1.667$, $p < 0.207$, ns). For the repeated measures ANOVA on Rotation Axis by Rotation Amount we also report results for analyses on 20 subjects because the statistical results for the important interaction below are the same as those for the 18 in the balanced design. The principle result from this analysis shown in Figure 5 presents the statistically significant interaction between Axis of Rotation and Amount of Rotation[3]. The differing effects of roll versus pitch or yaw axis was checked in a nonparametric analysis in which each participant's peak Movement Time across all rotations was ranked by Axis of Rotation. Participants' maxima were generally among rotations between 90° and 140°. A Friedman ANOVA on ranks confirmed that the greatest effects were for Roll: (Median ranks: Roll=1, Yaw=2, Pitch=3; $X^2(2)=6.10$, $p < 0.05$, Statistically identical results of PL omitted due to page limit).

DISCUSSION

Three main observations may be made as part of a descriptive data analysis. First, the MDF, i.e., the effect of the control-display rotation, is not isotropic w/r to axis of rotation, with roll having a distinctly larger nonlinearity and peak magnitude. We conjecture that these differences are due to the angle between the control-display rotation axis and the participant's two key body reference axes: the lateral left-right axis and the vertical axis usually aligned with gravity. Roll affects both unlike pitch and yaw. Our results using more generalized and isotropic 3D motion confirm some elements of Smith and Smith's (1962) suggestion that roll may be distinctly difficult. Replication with a prone participants could determine whether this difference relates to gravitational orientation.

Discussion of rotation axis anisotropies naturally leads to consideration of what are the most representative rotation parameters. Due consideration of the general nature of rotation immediately leads to the observation that besides the amount of rotation, the orientation of the rotation axis could a key model parameter to predict behavioral effects of rotations in general. We are currently collecting and analyzing new data from an experiment in which we carefully controlled our target locations and have preliminary evidence that target direction with respect to the rotation axis predicts aspects of performance. This analy-

[2] Though individual mean Path Length was highly correlated with mean Movement Time, this relation will not be discussed in the paper.

[3] Note the Axis X Rotation X Sequence interaction was: $F(90,252) = 1.215$, ns, so our Axis anisotropy finding also seems independent of Axis test order.

sis was not possible with the present data because of separate subject by subject random selection of target direction.

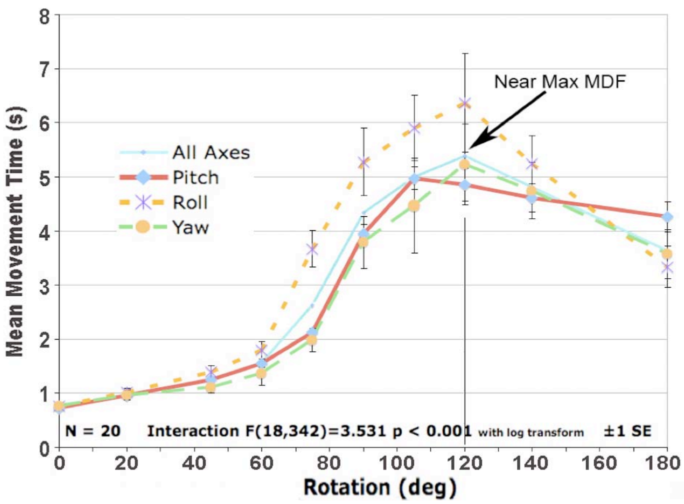

Figure 5. Interaction between Axis of Rotation and Amount of Rotation shows the MDF for each axis of rotation. The significant MDF across all three axes of rotation is also shown for reference as a thin blue path without error bars ($F(9, 171) = 108.45$, $p < 0.001$).

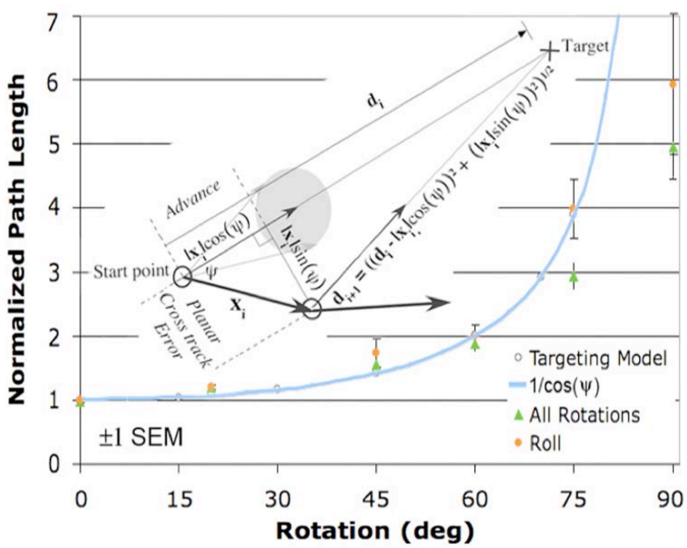

Figure 6. The first third of the MDF for rotation ψ in terms of Normalized Path Length (nPL) [4] and 1/cos(ψ). 1/cos(ψ) is the expected function if the paths are equiaxial spirals which they appear to be for $\psi < \sim 65°$. Since as $\psi \rightarrow 90°$, $nPL \rightarrow \infty$, further development will be needed to extend the theory and to discuss the effect of target direction.

A second important observation is not so much what we see present in the MDFs, but what is missing. Experiments on single-axis yaw misalignment have sometimes used flat, upright visual displays viewed perpendicularly with the comment, for example from Cunningham and Vardi (1990), that it is usually assumed that the 90° rotation in pitch does not substantially affect yaw misalignment. While we did not directly test their particular combination of pitch and yaw rotations, we cannot avoid noticing that our measure of the pitch MDF for 90° is not negligible; it is essentially equivalent to that of yaw or of the overall MDF. Probably a key factor at work is that in our experiment we tested fully 3D motion and only revealed the local frame of reference through visual motion cues. Other spatial cues such as the vertical surface of the display stereoscopically evident in Cunningham & Vardi (1990) or the explicit coordinate display used by Chintamani et al, (2010) are missing.

A final observation concerns the functional form of the MDF. Our measurements suggest its first 1/3 results is consistent with equiaxial spiral paths and that its maximum is between rotations of 105-120°. Why is it there? To answer such questions, we suggest extending our interative targeting model (Ellis & Adelstein, 2009). We have applied it successfully with a parameter-free fit to the first ~65° of rotation (Fig. 6) and hope to adapt it to explain why the MDF peaks and is different from other classical behavioral responses to rotated images, e.g., mental rotation (Shepard & Metzler, 1971) and discrimination of rotated faces (Collishaw & Hole, 2002).

Acknowledgments: NASA HRP Space Human Factors Engineering

References

Abeele, S. & Bock, O. (2001) Sensorimotor adaptation to rotated visual input: different mechanisms for small versus large rotations. *Exp. Brain Research, 140,* 407-410.

Chintamani, K. K., Cao, A. Ellis, R.D. & Pandya, A.K. (2010) Improved telemanipulator navigation during display-control misalignment using augmented reality cues. *IEEE Trans. Sys. Man & Cyber.(A). Sys. & Humans, 40*, 1, 29-39.

Collishaw, S.M. & Hole, G. J.(2002) Is there a linear or nonlinear relationship between rotation and configural processing. *Perception, 31*, 287-296.

Cunningham, H. & Vardi, I. (1990) Aiming error under transformed spatial mapping reveals spatial structure. *Biol. Cyber., 64,* 117-128.

Macedo, J.A., Kaber, D.B., Endsley, M.R., Powanusorn, P., & Myung, S. (1998) The effect of automated compensation for incongruent axes on teleoperator performance. *Human Factors, 40,* 4, 541-553.

Ellis, S. R., Tyler, M., Kim, W. S., & Stark, L. (1992) Three-dimensional tracking with misalignment between display and control axes. *SAE Trans.: J. of Aerospace, 100-1*, 985-989.

Ellis, S.R. & Adelstein, B.D. (2009) Kinesthetic compensation for sensorimotor rearrangements. *J. Motor Behavior, 41,* 6, 501– 518.

Fitts P. M . & Simon, C.W. (1952) Some relations between stimulus patterns and performance in a continuous dual-pursuit task *J. Exp.Psych.,43, 428-436*.

Jacoby, R.H., Adelstein, B.D., & Ellis, S.R. (1996) Improved temporal response in virtual environments through system hardware and software reorganization. Proc. of the SPIE, Stereoscopic displays and virtual reality systems, Vol. 2653, pp. 271-284.

Hill, M, Adelstein, B. D., & Ellis, S.R., (2004) Achieving minimum latency in virtual environment applications. Proc. of the 2004 Image Society.

Macedo, J.A., Kaber, D.B., Endsley, M.R., Powanusorn, P., & Myung, S. (1988) The effect of automated compensation for incongruent axes on teleoperator performance. *Human Factors, 40,* 4, 541-553.

Poulton, E.C. (1974) *Tracking & manual control*, Academic Press, New York.

Shepard, R & Metzler. J. (1971) Mental rotation of three dimensional objects. *Science, 171,* 972, 701-3.

Sheridan, T (2002) *Humans and automation*, Wiley, San Francisco, CA,.

Smith, K.U. & Smith W.M. (1962) *Perception and Motion,* Saunders, Philad.

Smith, T. J., Henning, R.A., & Li, Q. (1998). Teleoperation in space modeling effects of displaced feedback and microgravity on tracking performance. SAE Tech. Report No. 981701. Warrendale, PA.

Worringham, C. J. & Beringer, D. B. (1989). Operator orientation and compatibility in visual-motor task performance. *Ergonomics, 32*, 387-399.

Wickens, C.D., Keller, J.W. & Small, R.L. (2010): Left. No, Right Development of the Frame of Reference Transformation Tool (FORT). Proc. Human Factors & Ergonomics. Soc. 54th, pp. 1022-1026.

Yeom, K. Adelstein, B.D., & Ellis, S.R. (2012) Determining the discontinuities for three-dimensional trajectory data in teleoperation. Proc HFES, this volume.

[4] Normalized Path Length = mean Path Length / Target Distance .